ELSEVIER

Physica B 281&282 (2000) 673–674

PHYSICA B

www.elsevier.com/locate/physb

Local mode behavior in quasi-1D CDW systems

H. Fehske[a,*], G. Wellein[b], H. Büttner[a], A.R. Bishop[c], M.I. Salkola[d]

[a]*Physikalisches Institut, Universität Bayreuth, Universitatsstrasse 30, D-95440 Bayreuth, Germany*
[b]*Regionales Rechenzentrum Erlangen, Universität Erlangen, 91058 Erlangen, Germany*
[c]*MSB262, Los Alamos National Laboratory, Los Alamos, NM 87545, USA*
[d]*Superconductor Technologies Inc., Santa Barbara, CA 93111, USA*

Abstract

We analyze numerically the ground-state and spectral properties of the three-quarter filled Peierls–Hubbard Hamiltonian. Various charge- and spin-ordered states are identified. In the strong-coupling regime, we find clear signatures of local lattice distortions accompanied by intrinsic multi-phonon localization. The results are discussed in relation to recent experiments on MX chain [-PtCl-] complexes. In particular we are able to reproduce the observed red shift of the overtone resonance Raman spectrum.

Keywords: Charge density wave; Localized lattice distortions; Polarons; MX-chain compounds

Inspired by the recent observation of intrinsically localized vibrational modes in halide-bridged transition metal [-PtCl-] complexes [1], we study strong coupling effects between electronic and lattice degrees of freedom on the basis of a two-band, 3/4-filled Peierls–Hubbard model (PHM)

$$\begin{aligned}\mathscr{H} = & -t\sum_{\langle i,j\rangle\sigma} c_{i\sigma}^{\dagger}c_{\sigma j} + \sum_{i\sigma}\varepsilon_i n_{i\sigma} + \sum_i U_i n_{i\uparrow}n_{i\downarrow} \\ & + \lambda_{\mathrm{I}}(b_{\mathrm{I}} + b_{\mathrm{I}}^{\dagger})(n_1 + n_3 - n_2 - n_4) + \hbar\omega_{\mathrm{I}} b_{\mathrm{I}}^{\dagger}b_{\mathrm{I}}^{\dagger} \\ & + \lambda_{\mathrm{R}}(b_{\mathrm{R}} + b_{\mathrm{R}}^{\dagger})(n_2 - n_4) + \hbar\omega_{\mathrm{R}} b_{\mathrm{R}}^{\dagger}b_{\mathrm{R}}. \end{aligned} \quad (1)$$

In (1), the $c_{i\sigma}^{[\dagger]}$ are fermion operators, $n_{i\sigma} = c_{i\sigma}^{\dagger}c_{i\sigma}$, and $b_{\mathrm{R}}^{[\dagger]}$ and $b_{\mathrm{I}}^{[\dagger]}$ are the boson operators for the Raman active (R) and infrared (I) optical phonon modes with bare phonon frequencies ω_{R} and ω_{I}. With regard to the quasi-1D charge density wave (CDW) system $\{[\mathrm{Pt(en)_2}][\mathrm{Pt(en)_2Cl_2}](\mathrm{ClO_4})_4\}$ (en = ethylenediamine), subsequently abbreviated as PtCl, the Pt (Cl) atoms are denoted by the site index $i = 2, 4$ ($i = 1, 3$). The CDW state is built up by alternating nominal Pt^{+4} and Pt^{+2} sites with a corresponding distortion of Cl^{-}-ions towards Pt^{+4}. To model the situation of a 3/4-filled charge transfer insulator within a *single-mode approach* (SMA), we only include the R-(ν_1)-mode with $\hbar\omega_{\mathrm{R}} = 0.05$ [2], and parametrize the site energies by $\Delta = (\varepsilon_{\mathrm{Pt}} - \varepsilon_{\mathrm{Cl}})/t = 1.2$ and the Hubbard repulsions by $U_{\mathrm{Pt}} = 0.8$ and $U_{\mathrm{Cl}} = 0$ (all energies are measured in units of t). Alternatively, we employ a more realistic *double-mode approach* (DMA), using $\hbar\omega_{\mathrm{I}} = 0.06$ for the I-(ν_2)-mode [2].

The ground-state and spectral properties of the four-site PHM are determined by finite-lattice Lanczos diagonalization that preserves the full dynamics of the phonons [3].

Fig. 1 shows the variation of the lowest energy states as a function of the electron–phonon coupling. In the weak-coupling region, the ground-state is basically a zero-phonon state (cf. Fig. 2a) and the peaks in Fig. 1(a) correspond to multiples of the fundamental phonon frequency $\omega_{\mathrm{R}}^{(1)}$. As λ_{R} increases a strong mixing of electron and phonon degrees of freedom takes place, and finally the lowest states with total momentum $K = 0$ and π become nearly degenerate. In this limit a non-linear lattice potential stabilizing the so-called *intrinsically localized vibrational modes* (ILMs) is self-consistently generated [1].

A prominent feature of these bound states is their strong anharmonic redshift, resulting from the attractive interaction of Raman phonon quanta located at the same $\mathrm{PtCl_2}$ unit. The calculated red shift,

$$r_n = [n\omega_{\mathrm{R}}^{(1)} - \omega_{\mathrm{R}}^{(n)}]/\omega_{\mathrm{R}}^{(1)} \quad (2)$$

*Corresponding author. Fax: + 49-921-55-2991.
E-mail address: holger.fehske@theo.phy.uni-bayreuth.de (H. Fehske)

0921-4526/00/$ - see front matter
PII: S0921-4526(99)01066-2

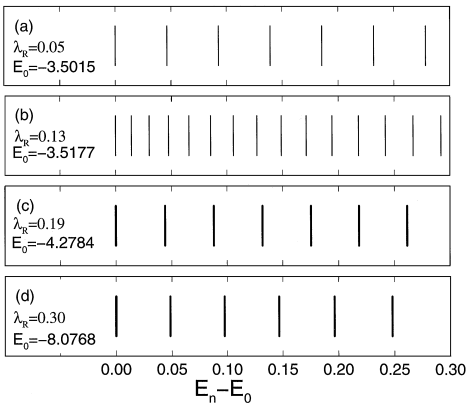

Fig. 1. Low-energy part of the eigenvalue spectrum of the PHM [periodic boundary conditions, SMA]. Eigenvalues in (c) and (d) are two-fold degenerate.

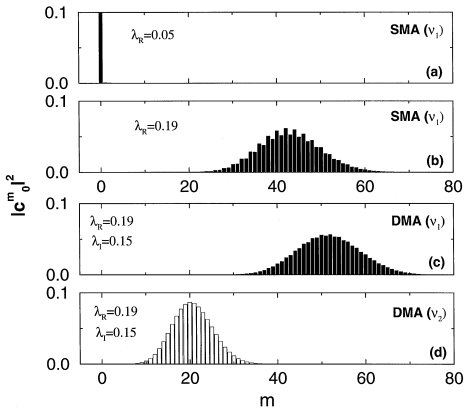

Fig. 2. Phonon distribution in the ground state for the antisymmetric I (white columns) and symmetric Cl-Pt-Cl stretch R (black columns) phonon modes.

Table 1
Relative red shift of the lowest-energy peaks in dependence on the final quanta of the vibrational energy [$\lambda_R = 0.33$; SMA]

r_n [%]	$n=$ 2	3	4	5	5	7
$Pt^{37}Cl$ [1]	0.4	1.1	2.4	4.6	7.7	11.6
SMA	0.4	1.3	2.8	4.8	7.5	10.9

with $\omega_R^{(n)} = (E_n - E_0)$, of the (doublet) overtones shown in Fig. 1(c) is successfully compared to experimental data probed by resonance Raman scattering (see Table 1). To elucidate the different nature of the ground state in the weak- and strong-coupling regimes, several characteristic quantities listed in Table 2. Obviously the self-localization transition is accompanied by significant changes in the spin and charge correlations. As can be seen from the weight of the m-phonon state in the ground state, $|c_0^m|^2$ [3], depicted in Fig. 2, the appearance of the ●-○-●-● configuration is related to large occupation numbers of the localized vibrational (R) mode.

Table 2
Different energy contributions to E_0, local particle densities [$\langle n_i \rangle$], local magnetic moments [$L_i = 3\langle (n_{i\uparrow} - n_{i\downarrow})^2 \rangle/4$], charge correlations [$\langle n_i n_j \rangle$] magnetic structure factor [$S_s(\pi) = 1/N \sum_{i,j} \langle S_i^z S_j^z \rangle e^{i\pi(i-j)}$] in the ground-state of the PHM. Note that the effect of Δ can be obtained dynamically within the DMA (see column 4)

	SMA		DMA	$\Delta = 0$
λ_I	0.0	0.0	0.15	0.15
λ_R	0.05	0.19	0.19	0.05
E_0	−3.5015	−4.2783	−5.3770	−3.2715
E_{kin}	−4.1115	−2.9186	−2.3202	−3.5985
E_{ph}	0.0001	2.1485	3.8490	0.2602
$E_{el\text{-}ph}$	−0.0036	−4.3026	−7.7017	−0.5433
E_U	0.6136	0.7945	0.7959	0.6102
$\langle n_{Cl} \rangle$	1.7047	1.8834	1.9561	1.7070
$\langle n_{Pt(2)} \rangle$	1.2953	0.2541	0.0949	1.2929
$\langle n_{Pt(4)} \rangle$	1.2953	1.9791	1.9929	1.2929
$\langle n_1 n_2 \rangle$	2.1053	0.3788	0.1441	2.1042
$\langle n_1 n_3 \rangle$	2.8611	3.5396	3.8253	2.8705
$\langle n_2 n_4 \rangle$	1.4990	0.4852	0.1824	1.4937
L_{Cl}	0.1897	0.0830	0.0323	0.1880
$L_{Pt(2)}$	0.3962	0.1696	0.0682	0.3977
$L_{Pt(4)}$	0.3962	0.0156	0.0053	0.3977
$S_s(\pi)$	0.1053	0.0524	0.0212	0.1042
Config.:	●-↑-●-↓	●-○-●-●	●-○-●-●	●-↑-●-↓

To summarize, the numerical results obtained for the PHM provide strong evidence for the existence of a dynamical spatial localization of vibrational energy (ILM) in MX solids, due to high intrinsic non-linearity from strong electron–lattice coupling.

References

[1] B.I. Swanson et al., Phys. Rev. Lett. 82 (1999) 3288.
[2] S.P. Love et al., Phys. Rev. B 47 (1993) 11107.
[3] B. Bäuml, G. Wellein, H. Fehske, Phys. Rev. B 98 (1998) 3663.